Biochemical Pharmacology 79 (2010) 552–564

Contents lists available at ScienceDirect

Biochemical Pharmacology

journal homepage: www.elsevier.com/locate/biochempharm

Cytotoxicity, cellular uptake, glutathione and DNA interactions of an antitumor large-ring Pt^{II} chelate complex incorporating the *cis*-1,4-diaminocyclohexane carrier ligand

Jana Kasparkova [a], Tereza Suchankova [a,b], Anna Halamikova [a], Lenka Zerzankova [a], Oldrich Vrana [a], Nicola Margiotta [c], Giovanni Natile [c], Viktor Brabec [a,*]

[a] Institute of Biophysics, Academy of Sciences of the Czech Republic, v.v.i., Kralovopolska 135, CZ-61265 Brno, Czech Republic
[b] Department of Experimental Physics, Faculty of Sciences, Palacky University, tr. 17. listopadu 12, 77146 Olomouc, Czech Republic
[c] Department of Pharmaceutical Chemistry, University of Bari, I-70125 Bari, Italy

ARTICLE INFO

Article history:
Received 26 June 2009
Accepted 18 September 2009

Keywords:
Antitumor
DNA damage
DNA repair
DNA polymerase
Glutathione
Platinum complex

ABSTRACT

Earlier studies have described promising antitumor activity of a large-ring chelate complex [$PtCl_2$(*cis*-1,4-DACH)] (DACH = diaminocyclohexane). Encouraging antitumor activity of this analogue of cisplatin prompted us to perform studies focused on the mechanistic basis of pharmacological effects of this complex. Four early steps in the mechanism of biological activity of cisplatin have been delineated: cell entry, reactions with sulfur-containing compounds, platinum–DNA binding along with processing platinated DNA by proteins (enzymes) and DNA repair. Here, we describe comparative experiments (involving also cisplatin) revealing: (i) improved cytotoxicity (3.4–5.4-fold) of [$PtCl_2$(*cis*-1,4-DACH)] in human tumor ovarian cell lines; (ii) enhanced cellular uptake (~1.5-fold) of [$PtCl_2$(*cis*-1,4-DACH)]; (iii) somewhat enhanced rate of reactions of [$PtCl_2$(*cis*-1,4-DACH)] with glutathione (~1.5-fold), but a similar rate of reactions with metallothionenin-2; (iv) enhanced rate of DNA binding of [$PtCl_2$(*cis*-1,4-DACH)] in cell-free media (~2-fold); (v) similar sequence preference of DNA binding of [$PtCl_2$(*cis*-1,4-DACH)] in cell-free media; (vi) identical DNA interstrand cross-linking efficiency (6%); (vii) similar bending (32°) and enhanced local unwinding (~1.5-fold) induced in DNA by the major 1,2-GG-intrastrand cross-link; (viii) markedly enhanced inhibiting effects of DNA adducts of [$PtCl_2$(*cis*-1,4-DACH)] on processivity of DNA polymerase; and (ix) a slightly lower efficiency of DNA repair systems to remove the adducts of [$PtCl_2$(*cis*-1,4-DACH)] from DNA.

1. Introduction

Serendipitous discovery of antitumor activity of cisplatin [*cis*-diamminedichloridoplatinum(II)] (Fig. 1B) and ensuing introduction of cisplatin, carboplatin [*cis*-diammine(cyclobutane-1,1-dicarboxylato)platinum(II)], nedaplatin [*cis*-diammine(glycolato)platinum(II)] and oxaliplatin {[(*1R,2R*-diaminocyclohexane)oxalato]platinum(II)] (diaminocyclohexane = DACH)} into the clinical use evoked a renaissance in inorganic chemistry and led to the synthesis and biological evaluation of many thousands of cisplatin analogues, and a thorough investigation of other nearby elements from the periodic table (for example, gold, osmium, palladium and ruthenium) [1,2]. Much of the early effort in the design of new platinum drugs was aimed at making cisplatin-based therapy safer to patients, in particular, lessening or removing unpredictable and severe nephrotoxicity and/or providing oral bioavailability. A second major, ongoing, initiative is to overcome tumor resistance to cisplatin, either that acquired during cycles of therapy with cisplatin (as

Abbreviations: bp, base pair; cisplatin, *cis*-diamminedichloridoplatinum(II); CFE, cell-free extract; CL, cross-link; CT, calf thymus; DACH, diaminocyclohexane; DEPC, diethyl pyrocarbonate; dNTP, deoxyribonucleoside 5′-triphosphate; DMSO, dimethylsulfoxide; DPP, differential pulse polarography; FAAS, flameless atomic absorption spectrophotometry; GSH, glutathione; HPLC, high-pressure liquid chromatography; IC_{50}, concentration inhibiting cell growth by 50%; KF^-, Klenow fragment from DNA polymerase I (exonuclease minus mutated to remove the 3′→5′ proofreading domain); MT, metallothionein; MT-2, metallothionein isoform MT-2; oxaliplatin, [Pt(oxalate)(*1R,2R*-DACH)]; PAA, polyacrylamide; r_b, the number of molecules of the Pt^{II} complex bound per nucleotide residue; r_i, the molar ratio of free metal complex to nucleotide phosphates at the onset of incubation with DNA; $t_{1/2}$, half time; transplatin, *trans*-diamminedichloridoplatinum(II).

* Corresponding author. Tel.: +420 541517148; fax: +420 541240499.
E-mail address: brabec@ibp.cz (V. Brabec).

0006-2952/$ – see front matter © 2009 Elsevier Inc. All rights reserved.
doi:10.1016/j.bcp.2009.09.019

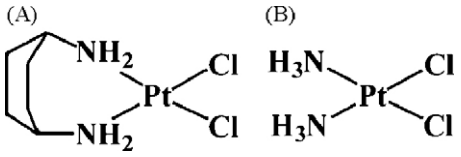

Fig. 1. Structures of [$PtCl_2$(*cis*-1,4-DACH)] (A) and cisplatin (B).

occurs in patients with, for example, ovarian cancer [3,4]) or intrinsic resistance (such as that seen in patients with, for example, colorectal, prostate, lung or breast cancer [5–7]).

Cisplatin and its analogues bind to various cellular components like DNA, RNA, proteins, and membrane phospholipids. The important target leading to cell death is genomic DNA [8–10], although targets other than DNA may be also important for these agents [11–13]. Nevertheless, it is generally accepted that an important feature of mechanism of action of cisplatin and its analogues is their binding to nuclear DNA and subsequent blockage of transcription while eluding repair [14–17].

Cisplatin, carboplatin and nedaplatin form in DNA the same major 1,2-GG intrastrand cross-links (CLs) [15], whereas DNA intrastrand and interstrand CLs of oxaliplatin are different [18,19] and may account in part for its different spectrum of activity observed in combination with 5-fluorouracil/leucovorin. Success of oxaliplatin, which incorporates the *1R,2R*-DACH carrier ligand as Pt^{II} complex, raised considerable research interest over the past three decades in platinum–DACH complexes. Thus, in a search for more effective platinum antitumor complex that is also capable of overcoming cisplatin resistance *in vivo* a large-ring chelate complex [$PtCl_2$(*cis*-1,4-DACH)] (Fig. 1A) was synthesized and tested for cytotoxicity in tumor cell lines and for antitumor activity against the murine leukemias and human solid tumors [20]. Interestingly, this analogue features a mode of metal–ligand chelation in which the *cis*-1,4-DACH ligand is bonded to Pt^{II} in a locked boat conformation.

The *cis*-[$PtCl_2$(1,4-DACH)] complex has shown great clinical promise [20–22]. The findings that it exhibits better *in vitro* cytotoxicity than cisplatin [20] and also has substantial *in vivo* activity in L1210 leukemia cell lines resistant to oxaliplatin suggest that differences in shape or conformation of platinum complexes are important in eliciting the antitumor activity of [$PtCl_2$(*cis*-1,4-DACH)] complex [21,22]. These results have been interpreted to mean [23] that the [$PtCl_2$(*cis*-1,4-DACH)] complex is neither a cisplatin- nor a [$PtCl_2$(*1R,2R*-DACH)]-type analogue but rather a system that incorporates properties of both. Hence, the encouraging antitumor activity of [$PtCl_2$(*cis*-1,4-DACH)] coupled with a considerably enhanced aqueous solubility compared to [$PtCl_2$(*1R,2R*-DACH)] is an impetus for studies focused on the mechanistic basis of biological (pharmacological) effects of this complex.

The first mechanistic studies focused on unique antitumor effects of [$PtCl_2$(*cis*-1,4-DACH)] were performed only recently [23,24]. These studies have revealed that the [$PtCl_2$(*cis*-1,4-DACH)] forms a seven-member chelating ring with platinum, which leads to considerable strain during bidentate [$PtCl_2$(*cis*-1,4-DACH)] binding. Moreover, in [$PtCl_2$(*cis*-1,4-DACH)], the N-Pt-N bite angle (97°) is much larger than those found in other Pt^{II} complexes with bidentate diamines or in cisplatin (91°). Such a large angle could enhance the steric interactions between cis purine residues in bifunctional adducts of [$PtCl_2$(*cis*-1,4-DACH)]. These recent results led to the hypothesis that [$PtCl_2$(*cis*-1,4-DACH)] forms DNA adducts having the conformation different from that of DNA adducts of cisplatin or oxaliplatin. As DNA is considered the major pharmacological target of cisplatin and its analogues [14,16], the proposed difference in DNA binding mode of [$PtCl_2$(*cis*-1,4-DACH)] has been suggested to be associated at least in part with more favorable biological (pharmacological) effects of 1,4-DACH analogue [23,24].

A primary objective in the present work was to understand more fully the molecular mechanism of action of [$PtCl_2$(*cis*-1,4-DACH)]. Four early steps in the mechanism of biological activity of cisplatin and its analogues have been delineated, namely: cell entry, reactions with sulfur-containing compounds, platinum–DNA binding and processing of platinated DNA by proteins (enzymes) and DNA repair. Here, we describe experiments revealing (i) cytotoxicity of [$PtCl_2$(*cis*-1,4-DACH)] in human ovarian cell lines A2780 and A2780cisR (sensitive and resistant to cisplatin, respectively), i.e. in the tumor cell lines most frequently used to test cytotoxicity of cisplatin and its analogues, (ii) cellular uptake of [$PtCl_2$(*cis*-1,4-DACH)], (iii) DNA binding mode of [$PtCl_2$(*cis*-1,4-DACH)] in cell-free media, (iv) effects of DNA adducts of [$PtCl_2$(*cis*-1,4-DACH)] on processivity of DNA polymerase, and (v) repair of DNA adducts of [$PtCl_2$(*cis*-1,4-DACH)].

2. Materials and methods

2.1. Chemicals

[$PtCl_2$(*cis*-1,4-DACH)] was prepared as described previously [24]. Purity of [$PtCl_2$(*cis*-1,4-DACH)] was higher than 95% as established by combustion analysis carried out with a Hewlett Packard 185 C, H, and N analyzer. Cisplatin and *trans*-diamminedichloridoplatinum(II)] (transplatin) were obtained from Sigma (Prague, Czech Republic) (purity was ≥99.9% based on elemental and ICP trace analysis). The stock solutions of platinum compounds were prepared at the concentration of 5×10^{-4} M in 10 mM $NaClO_4$ and stored at 4 °C in the dark. Calf thymus (CT) DNA (42% G + C, mean molecular mass ca. 20 000 kDa) was prepared and characterized as described previously [25,26]. Plasmids pSP73KB [2455 base pairs (bp)] and pSP73 (2464 bp) were isolated according to standard procedures. The synthetic oligodeoxyribonucleotides were synthesized and purified as described previously [27]. T4 DNA ligase, Klenow fragment from DNA polymerase I (exonuclease minus, mutated to remove the 3′ → 5′ proofreading domain) (KF^-), restriction endonucleases EcoRI, HindIII, NdeI, SspI, Circum Vent™ Thermal Cycle Sequencing Kit with Vent(exo^-) DNA polymerase and T4 polynucleotide kinase were purchased from New England Biolabs (Beverly, MA). Deoxyribonucleoside 5′-triphosphates (dNTPs) were from Roche Diagnostics, GmbH (Mannheim, Germany). Agarose was from FMC BioProducts (Rockland, ME). Acrylamide, bis(acrylamide), ethidium bromide (EtBr), urea and NaCN were from Merck KgaA (Darmstadt, Germany). Dimethyl sulfate, $KMnO_4$, diethyl pyrocarbonate (DEPC), glutathione (GSH), KBr and $KHSO_5$ were from Sigma (Prague, Czech Republic). Proteinase K, ATP and dNTPs were from Boehringer (Mannheim, Germany). Rabbit metallothionenin isoform designated MT-2 (Zn7-MT-2) was a kind gift of Prof. M. Vasak (University of Zurich, Zurich, Switzerland). Radioactive products were from Amersham (Arlington Heights, IL, USA). A cell-free extract (CFE) was prepared from the repair proficient HeLa S3 cell line as described [28,29]. Taq polymerase and Q solution were from Qiagen (BIO-CONSULT spol. s.r.o., Prague, Czech Republic). Sybr-Green® was from Molecular Probes (Leiden, The Netherlands).

2.2. Cytotoxicity

Cisplatin and [$PtCl_2$(*cis*-1,4-DACH)] were dissolved in dimethylsulfoxide (DMSO). The stock solutions (100 mM) of the Pt compounds in DMSO were diluted with the aqueous cell culture medium in several steps immediately after their dissolution in DMSO. The final concentration of DMSO in cell culture medium did not exceed 0.25%. The A2780 (parent cisplatin sensitive) and

A2780cisR (with acquired cisplatin resistance) human ovarian carcinoma cell lines were grown in RPMI 1640 medium (GIBCO) supplemented with gentamycin (50 μg/mL, Serva) and 10% heat inactivated fetal bovine serum (GIBCO). The acquired resistance of A2780cis cells was maintained by supplementing the medium with 1 μM cisplatin every second passage. The cells were cultured in a humidified incubator at 37 °C in a 5% CO_2 atmosphere and subcultured 2–3 times a week with an appropriate plating density. The cells were seeded in 96-well tissue cultured plates at a density of 10^4 cells/well. After overnight incubation (16 h), the cells were treated with the platinum compounds. After 72 h of incubation 10 μL of a freshly diluted 3-(4,5-dimethyl-2-thiazolyl)-2,5-diphenyl-2H-tetrazolium bromide (MTT) solution (2.5 mg/mL) were added to each well and the plate was incubated at 37 °C in a humidified 5% CO_2 atmosphere for 4 h. At the end of the incubation period the medium was removed and the formazan product was dissolved in 50 μL of DMSO. The cell viability was evaluated by measurement of the absorbance at 570 nm, using an Absorbance Reader SUNRICE TECAN SCHOELLER. IC_{50} values (compound concentration that produces 50% of cell growth inhibition) were calculated from curves constructed by plotting cell survival (%) versus drug concentration (μM). All experiments were made in quadruplicate. The reading values were converted to the percentage of control (% cell survival). Cytotoxic effects were expressed as IC_{50} values.

2.3. Cellular platinum uptake

Cellular uptake of [$PtCl_2$(*cis*-1,4-DACH)] and cisplatin was measured in A2780 cells (sensitive to cisplatin). The cells were seeded in 60 mm tissue culture dishes (30 000 per cm^2). After overnight incubation, the cells were treated with the platinum compound for 4 or 24 h at the concentrations of 2.7 μM. The cell monolayers at the end of the incubation with the Pt complex were washed (twice) with ice-cold phosphate buffered saline (PBS), trypsinized and harvested into cold (4 °C) PBS. Cell suspensions were centrifuged and the pellets were stored in PBS at −80 °C until assayed. Afterward, the pellets were digested with 12 M HCl and platinum content determined by flameless atomic absorption spectrophotometry (FAAS). The results of cellular platinum uptake were corrected for adsorption effects [30]. All experiments were made in quadruplicate.

2.4. Reactions with sulfur-containing compounds

Reactions of GSH and mammalian MT-2 with [$PtCl_2$(*cis*-1,4-DACH)] and cisplatin were investigated by monitoring UV absorption at 260 nm of solutions containing the platinum complex and GSH or MT-2 exactly as described in the previous work [31,32]; the absorbance at 260 nm reflects the presence of platinum–sulfur and disulfide bonds. The platinum compounds (from aged stock solutions equilibrated in 10 mM $NaClO_4$) were mixed with GSH or MT-2 at 37 °C in the medium of 10 mM $NaClO_4$ plus 0.1 mM phosphate buffer, pH 7.0, in the dark. Reactions were initiated by mixing the platinum complex with the buffer followed by immediate addition of GSH or MT-2. The experiments were made in triplicate. The kinetic data were fitted by non-linear regression (GraphPad Prism) to one-phase and two-phase exponential association. The decision as to which fit was more appropriate for each dependence was made by comparing the fits of the two equations by using an *F*-test (GrahPad Prism).

2.5. Platination reactions in cell-free media

CT or plasmid DNAs were incubated with the platinum complex in 10 mM $NaClO_4$ at 37 °C in the dark. After 24 h, the samples were exhaustively dialyzed against the medium required for subsequent biochemical or biophysical analysis. An aliquot of these samples was used to determine the value of r_b by FAAS, or by differential pulse polarography (DPP) [33].

The duplexes containing single, central 1,2-GG intrastrand CL of *cis*-$[Pt(1,4\text{-DACH})]^{2+}$ or cisplatin in the pyrimidine-rich top strands were prepared as described [27,34]. The platinated oligonucleotides were purified by ion-exchange high-pressure liquid chromatography (HPLC). It was verified by platinum FAAS and by the measurements of the optical density that the modified oligonucleotides contained one platinum atom. It was also verified using dimethyl sulfate footprinting of platinum on DNA [34,35] that one [$PtCl_2$(*cis*-1,4-DACH)] or cisplatin molecule was coordinated to the N7 atoms of the two Gs in the top strands of each duplex. Other details have been described previously [27,36].

2.6. Sequence preference of DNA adducts

The primer extension footprinting assay was used to evaluate the sequence selectivity of DNA modification by [$PtCl_2$(*cis*-1,4-DACH)] in comparison to cisplatin and transplatin. The fragment of pSP73 DNA linearized by HpaI (2464 bp) was incubated with platinum complexes in 10 mM $NaClO_4$ for 24 h at 37 °C to obtain r_b = 0.005 (r_b = the number of molecules of the Pt^{II} complex bound per nucleotide residue). The excess of drug was removed by ethanol precipitation. Circum Vent™ Thermal Cycle Sequencing Kit with Vent(exo$^-$) DNA polymerase was used along with the protocol for thermal cycle DNA sequencing with 5′ end-labeled 20-mer SP6 primer recommended by the manufacturer with small modifications [37]. The synthesis products were separated by electrophoresis on a denaturing polyacrylamide (PAA) gel (6% PAA/8 M urea); sequence ladders were obtained in parallel using untreated control DNA fragment.

2.7. Interstrand cross-link assay

The [$PtCl_2$(*cis*-1,4-DACH)] complex at varying concentrations were incubated for 24 h with 500 ng of pSP73KB DNA after it had been linearized by EcoRI and 3′-end labeled by means of KF^- and [α-^{32}P]dATP. The amount of interstrand CLs was analyzed by electrophoresis under denaturing conditions on alkaline agarose gel (1%). After the electrophoresis was completed, the intensities of the bands corresponding to single strands of DNA and interstrand cross-linked duplex were quantified. The frequency of interstrand CLs, %ICL/Pt (the number of interstrand CLs per adduct), was calculated as $\%ICL/Pt = XL/4910 \cdot r_b$ (pSP73KB plasmid contained 4910 nucleotide residues) [35]. XL is the number of interstrand CLs per molecule of the linearized DNA duplex which was calculated assuming Poisson distribution of the interstrand CLs as $XL = -\ln A$, where A is the fraction of molecules running as a band corresponding to the non-cross-linked DNA.

2.8. Unwinding of negatively supercoiled DNA

Unwinding of closed circular supercoiled pSP73KB plasmid DNA was assayed by an agarose gel mobility shift assay [38]. The unwinding angle Φ, induced per Pt–DNA adduct was calculated upon the determination of the r_b value at which the complete transformation of the supercoiled to relaxed form of the plasmid was attained. Samples of pSP73KB plasmid were incubated with platinum compounds at 37 °C in the dark for 24 h. The samples were subsequently subjected to electrophoresis on 1% agarose gels running at 25 °C in the dark with TAE (Tris-acetate/EDTA) buffer. The gels were then stained with EtBr, followed by photography with transilluminator.

2.9. Chemical modifications

The modification by $KMnO_4$, DEPC and $KBr/KHSO_5$ were performed as described previously [27,39–41]. The strands of the 22-bp duplex TGGT(22) (its nucleotide sequence is shown in Fig. S2A) were 5′-end-labeled with [γ-^{32}P]ATP. In the case of the platinated oligonucleotides, the platinum complex was removed after reaction of the DNA with the probe by incubation with 0.2 M NaCN (pH 11) at 45 °C for 10 h in the dark.

2.10. Ligation and electrophoresis of oligonucleotides

Unplatinated 19–23-mer single strands (bottom strands of the duplexes shown in Fig. S2A) were 5′-end-labeled with [γ-^{32}P]ATP by using T4 polynucleotide kinase. Then they were annealed with their phosphorylated complementary strands (unplatinated or containing the platinum CL). The duplexes were allowed to react with T4 DNA ligase. The resulting samples along with ligated unplatinated duplexes were subsequently examined on 8% native PAA [mono:bis(acrylamide) ratio = 29:1] electrophoresis gels. Other details of these experiments were as described in previous papers [42–44].

2.11. Inhibition of DNA polymerization

The primer extension assays with all four dNTPs were performed with the 23-mer templates containing a single 1,2-GG intrastrand adduct of *cis*-[Pt(1,4-DACH)]$^{2+}$ or cisplatin which were prepared in the same way as described in Section 2.5. DNA substrates were generated by annealing the 23-mer template containing site-specific adducts of [$PtCl_2$(*cis*-1,4-DACH)] or cisplatin to the 12- or 16-mer 5′-^{32}P labeled oligomer primers. In the control undamaged DNA substrates, nonplatinated 23-mer template was used. The sequences of DNA substrates containing 23-mer template oligonucleotides annealed to the primers are shown in Fig. 5. Standard DNA polymerase (KF^-) reactions (50 μL) contained 50 mM Tris–HCl (pH 7.4), 10 mM $MgCl_2$, 0.1 mM dithiothreitol, 50 μg/mL bovine serum albumin, 100 μM dNTPs, 20 nM 5′-^{32}P labeled oligonucleotide primer annealed to an oligonucleotide template and 0.5 unit of KF^- (6 nM). After incubation for certain time at 25 °C, aliquots (10 μL) were withdrawn and the reactions in these aliquots were terminated by the addition of 5 μL of loading buffer containing 20 mM EDTA, 95% formamide, 0.3% bromphenol blue and 0.3% xylenecyanol blue and by heating at 90 °C for 1 min. The reaction products were resolved on 24% PAA gels containing 8 M urea and then visualized and quantified. Other details were published previously [45,46].

Steady-state kinetic analysis for dCTP incorporation opposite the 3′ platinated G involved in the 1,2-GG intrastrand CL of cisplatin or [$PtCl_2$(*cis*-1,4-DACH)] or this G contained in the unplatinated template catalyzed by KF^- was done as described previously [47–50]. Briefly, KF^- was incubated with DNA substrates generated by annealing the 23-mer template containing site-specific adducts of [$PtCl_2$(*cis*-1,4-DACH)] or cisplatin to the 16-mer 5′-^{32}P labeled oligomer primer (Fig. S3) with increasing concentration of dCTP (in the absence of other deoxyribonucleotide triphosphates) for 5 min under standard reaction conditions (*vide supra*). Gel band intensities of the substrates and products were visualized and quantified. The percentage of primer extended (the sum of the integrated intensities of bands corresponding to all products 17 or more nucleotides long [47–50]) was plotted as a function of dCTP concentration, and the data were fitted by non-linear regression using GraphPad software to the Michaelis–Menten equation describing hyperbola, $v = (V_{max} \times [dCTP]/K_m + [dCTP])$. Apparent K_m and V_{max} steady-state parameters were obtained from the best fit and were used to calculate the efficiency of the dCTP insertion opposite the template 1st (3′) platinated G to the efficiency of the dCTP insertion opposite this G which was unplatinated [$(V_{max}/K_m)_{platinated\ template}/(V_{max}/K_m)_{unplatinated\ template}$].

2.12. DNA repair synthesis by human cell extract

DNA repair synthesis of CFEs of DNA repair proficient HeLa cells was assayed as described previously [51–53] using pSP73 plasmid. Each reaction of 50 μL contained 600 ng of nonmodified or platinated pSP73, 2 mM ATP, 30 mM KCl, 0.05 mg/mL rabbit muscle creatine phosphokinase, 20 mM of each dGTP, dATP and TTP, 8 mM dCTP, 74 kBq of [α-^{32}P]dCTP in the buffer composed of 40 mM HEPES–KOH, pH 7.5, 5 mM $MgCl_2$, 0.5 mM dithiothreitol, 22 mM creatine phosphate, 70 mM potassium glutamate, 1.4 mg bovine serum albumin/mL and 20 μg of HeLa CFE. Reactions were incubated for 4 h at 30 °C and terminated by adding EDTA to a final concentration of 20 mM, SDS to 0.6% and proteinase K to 250 μg/mL and then incubating for 30 min. The products were extracted with 1 volume of 1:1 phenol:chloroform. The DNA was precipitated from the aqueous layer by the addition of 0.1 volume of 3 M sodium acetate and 2.5 volumes of ethanol. After 30 min of incubation at −20 °C and centrifugation at 12,000 × *g* for 30 min at 4 °C, the pellet was washed with 0.2 mL 70% ethanol and dried. DNA was finally linearized by SspI (which cuts only once within pSP73 plasmid) before electrophoresis on a 1% agarose gel. The resulting gel was stained by SybrGreen® according to the manufacturer's protocol and the radioactivity associated with the bands was quantitated. The experiments were made in quadruplicate.

2.13. DNA repair in cells

Detection of gene-specific repair in cells was performed as described previously [54–56]. Briefly, A2780 cells were treated with [$PtCl_2$(*cis*-1,4-DACH)] and cisplatin (200 μM) for 5 h, followed by treatment with 0.1 M thiourea for 1 h to block the conversion of monoadducts to CLs during the post-treatment incubation. The cells were then incubated for times up to 6 h in drug-free medium. Cells were harvested, total genomic DNA was isolated and the DNA concentration of the samples was determined by UV spectrophotometry. The DNA was then restriction-digested with HindIII at 37 °C for 2 h, and extracted using phenol/chloroform followed by ethanol precipitation. The pellet was resuspended in TE buffer (10 mM Tris, pH 8.0, 1 mM EDTA), the final DNA concentration recovered was determined as described above and quantitative PCR of an 1858-bp fragment of the *DHFR* gene was performed. Each PCR amplification mixture (25 μl) consisted of 150 ng of total genomic DNA and contained 0.625 U of Taq polymerase Qiagen, primers (0.5 μM for each primer; sense primer, 5′-ACGTAGCTCGTCCTCAAA, antisense primer, 5′-GCACTGGTAAACTTCATCAAG, dNTPs (0.2 mM each), 1× Qiagen PCR buffer, 1× Q solution (Qiagen), 2.6 mM $MgCl_2$, and made up to 25 μL with Milli-Q water. The PCR conditions employed involved an initial denaturation at 96 °C for 5 min, 29 cycles of 96 °C for 1 min, 58 °C for 1 min, 72 °C for 1.5 min, and a final equilibration for 5 min at 72 °C. The amplification products were then resolved on a 1% agarose gel in 1× Tris/acetate/EDTA buffer, pH 7.0. The gel was then stained with SyberGreen, then destained in water and the bands were quantitated. The Poisson distribution was used to calculate the number of adducts in the amplified fragment of the gene and the repair efficiency was expressed as the percentage of initial adducts that remained at that time point.

2.14. Other physical methods

Absorption spectra were measured with a Beckman 7400 DU spectrophotometer and quartz cells with a thermoelectrically controlled cell holder and quartz cells with a path length of 1 cm. Purification of oligonucleotides with the aid of HPLC was carried

out on a Waters HPLC system consisting of Waters 262 pump, Waters 2487 UV detector, and Waters 600S controller with MonoQ HR 5/50 GL column. The FAAS measurements were carried out on a Varian AA240Z Zeeman atomic absorption spectrometer equipped with a GTA 120 graphite tube atomizer. For FAAS analyses, DNA was precipitated with ethanol and dissolved in HCl (0.1 M). DPP was performed with an EG&G Princeton Applied Research Corporation Model 384B Polarographic Analyzer. The gels were visualized by using a BAS 2500 FUJIFILM bioimaging analyzer, and the radioactivity associated with bands was quantitated with the AIDA image analyzer software (Raytest, Germany).

3. Results

3.1. Cytotoxicity

The cytotoxic activity of the [$PtCl_2$(*cis*-1,4-DACH)] complex tested in the present work was determined against A2780 (parent cisplatin sensitive) and A2780cisR (with acquired cisplatin resistance) human ovarian carcinoma cell lines, commonly used to test cytotoxic activity of cisplatin analogues and other antitumor metallodrugs. A2780cisR cells are resistant to cisplatin through a combination of decreased uptake, enhanced DNA repair/tolerance, and elevated reduced glutathione levels [57]. The tumor cell lines were incubated for 72 h with the platinum compounds and the cell survival in the culture treated with the platinum compounds was evaluated as described in Section 2.2. Results (Table 1) show that [$PtCl_2$(*cis*-1,4-DACH)] is significantly more cytotoxic than cisplatin. Interestingly, the cytotoxicity of [$PtCl_2$(*cis*-1,4-DACH)] in the cisplatin-resistant line A2780cisR is characterized by lower value of resistance factor (Table 1).

3.2. Cellular uptake

The factor that is usually thought to contribute to platinum drug cytotoxicity is also cellular uptake. To examine accumulation of [$PtCl_2$(*cis*-1,4-DACH)], the cellular levels of this compound were measured after a short (4 h) or long time (24 h) exposure of the A2780 cells to the drugs. Consistent with its enhanced cytotoxicity, the uptake of [$PtCl_2$(*cis*-1,4-DACH)] was approximately 1.3–2-fold greater than that of cisplatin (Table 1).

3.3. Reactions with sulfur-containing compounds

Pt^{II} compounds have a strong thermodynamic preference for binding to sulfur donor ligands. Hence, before antitumor platinum drugs reach DNA in the nucleus of tumor cells, they may interact with various compounds, including sulfur-containing molecules. These interactions are generally thought to play a role in mechanisms underlying tumor resistance to platinum compounds, their inactivation, and their side effects [58]. Therefore, interest in the interactions of platinum antitumor drugs with sulfur-containing molecules of biological significance has recently increased markedly. Examples of endogenous thiols to which platinum complexes bind when they are administered intravenously or after they enter the cell are GSH and metallothioneins (MTs). MTs are small (~6–7-kDa) cellular metalloproteins that strongly bind metal ions. The metal ion binding domains of MT isoform designated MT-2 consist of 20 cysteine residues arranged in two thiol (S)-rich sites [59].

In the present work, we investigated reactions of GSH and mammalian MT-2 with [$PtCl_2$(*cis*-1,4-DACH)] and cisplatin using UV absorption spectrophotometry [31,32]. [$PtCl_2$(*cis*-1,4-DACH)] or cisplatin at a concentration of 33 μM was mixed with 5 mM GSH (this concentration of GSH is physiologically relevant [59]) at 37 °C. The $t_{1/2}$ (half-times of the reactions), which mainly result in the formation of platinum–sulfur bonds, were 58 ± 3 and 88 ± 4 min for reactions of [$PtCl_2$(*cis*-1,4-DACH)] and cisplatin with GSH, respectively (one-phase exponential association). Thus, [$PtCl_2$(*cis*-1,4-DACH)] reacted with GSH with a somewhat faster rate than cisplatin. [$PtCl_2$(*cis*-1,4-DACH)] or cisplatin at the concentration of 200 μM were also mixed with MT-2 at the concentration of 2.1 μM under the same conditions. The half-times of the reaction of

Table 1
Summary of the effects of [$PtCl_2$(*cis*-1,4-DACH)] and cisplatin on tumor cells, DNA and sulfur-containing compounds observed in this work.

	[$PtCl_2$(*cis*-1,4-DACH)]	Cisplatin
IC_{50} (μM) in A2780 cells[a]	0.8 ± 0.2	2.7 ± 0.6
IC_{50} (μM) in A2780cisR cells[a,b]	4.0 ± 0.9 (5)	21.6 ± 4.5 (8)
Uptake by A2780 cells (pmol Pt/10^6 cells)[c]		
After 4 h treatment	4.7 ± 0.9	3.1 ± 0.2
After 24 h treatment	38 ± 3	22 ± 5
Reaction with GSH, $t_{1/2}$ (min)[d]	58 ± 3	88 ± 4
Reaction with MT-2, $t_{1/2}$ (min)[d]	212 ± 5	224 ± 6
DNA binding ($t_{50\%}$) (min)[d]	65 ± 8	120[e]
Preferential DNA binding sites[d,f]	GG, AG	GG, AG
% interstrand CLs/adduct[d]	6 ± 1	6[g]
Plasmid DNA unwinding angle/adduct[d]	15 ± 2°	13°[h]
DNA unwinding angle/1,2-GG intrastrand CL[d]	19 ± 2°	13 ± 3°[i]
DNA bending angle/1,2-GG intrastrand CL[d]	33 ± 1°	32°[j]
Reactivity of chemical probes around the 1,2-GG intrastrand CL[d,k]		
Inhibition of DNA polymerization by the 1,2-GG intrastrand CL[d]	High	Low
DNA repair synthesis (%)[d]	85	100

[a] Drug treatment period was 72 h.
[b] Resistance factor, defined as IC_{50}(resistant)/IC_{50}(sensitive), is given in parentheses.
[c] Cells were treated with the Pt complex at the concentration of 2.7 μM.
[d] See the text for details.
[e] Ref. [61].
[f] Determined by replication mapping.
[g] Ref. [35].
[h] Ref. [38].
[i] Ref. [91].
[j] Ref. [43].
[k] Summary of the reactivity of chemical probes; full and open circles designate strong or weak reactivity, respectively.

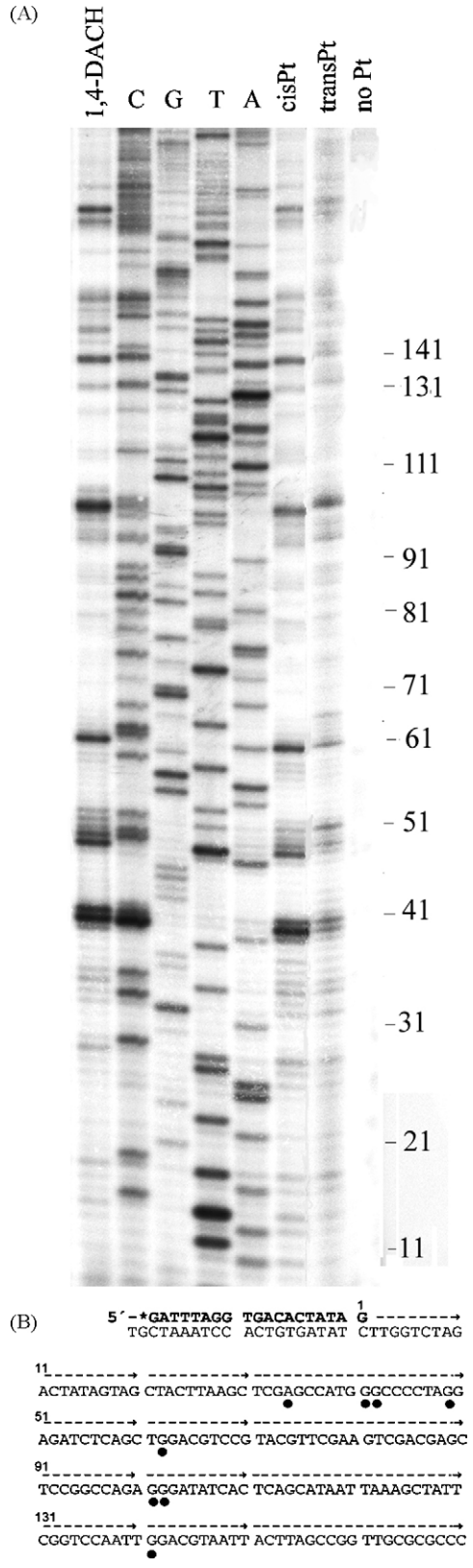

Fig. 2. Sequence preference of DNA adducts. (A) Autoradiogram of 6% polyacrylamide/8 M urea sequencing gel showing inhibition of DNA synthesis by VentR(exo$^-$) DNA polymerase on the pSP73 plasmid DNA linearized by HpaI restriction enzyme and subsequently modified by platinum complexes. The gel contained the linear amplification products of control, nonplatinated DNA, and DNA treated with [$PtCl_2$(*cis*-1,4-DACH)], cisplatin or transplatin at r_b = 0.005. Lanes are as follows: (control) unmodified template; lanes 1,4-DACH, cisPt and transPt, DNA modified by [$PtCl_2$(*cis*-1,4-DACH)], cisplatin or transplatin, respectively; lanes C, G, T, A, chain-terminated marker DNAs (note that these dideoxy sequencing lanes give the sequence complementary to the template strand). The numbers correspond to the nucleotide sequence numbering of part (B). Schematic diagram showing a portion of the sequence used to monitor inhibition of DNA synthesis on the template containing adducts of [$PtCl_2$(*cis*-1,4-DACH)]. The arrows indicate the direction of the synthesis. Circles indicate major stop signals from part (A), lane 1,4-DACH. The numbering of the nucleotides in this scheme corresponds to the numbering of the nucleotides in the pSP73 nucleotide sequence map.

[$PtCl_2$(*cis*-1,4-DACH)] or cisplatin with MT-2 (one-phase exponential association) were similar (212 ± 5 or 224 ± 6 min, respectively).

3.4. DNA modification in a cell-free medium

3.4.1. DNA binding

One of the important early phases of the mechanism by which platinum compounds exert their anticancer activity is formation of adducts on nuclear DNA by these agents [16,17,60]. Hence, data on DNA binding mode of platinum complexes are of great interest. In the present study, we have applied some methodologies previously developed for cisplatin and its analogues to investigate the reaction products of [$PtCl_2$(*cis*-1,4-DACH)] with DNA in cell-free media.

In order to determine the character of DNA adducts of [$PtCl_2$(*cis*-1,4-DACH)] we examined the DNA binding properties of this complex and compared these binding properties with those of parent cisplatin. The first experiments were aimed at quantifying the binding of [$PtCl_2$(*cis*-1,4-DACH)] to mammalian DNA. Solutions of double-helical CT DNA at a concentration of 0.056 mg/mL were incubated with [$PtCl_2$(*cis*-1,4-DACH)] at the value of r_i of 0.05 in 10 mM $NaClO_4$ at 37 °C (r_i is defined as the molar ratio of free platinum complex to nucleotide phosphates at the onset of incubation with DNA). At various time intervals, an aliquot of the reaction mixture was withdrawn and assayed by DPP for platinum not bound to DNA. No changes in the pH of the reaction mixture containing DNA and platinum compounds were measured within 48 h after mixing DNA with the platinum complex. The amount of the platinum compound bound to DNA increased with time. In this binding reaction the time at which the binding reached 50% ($t_{50\%}$) was 65 ± 8 min (Table 1). Thus, the [$PtCl_2$(*cis*-1,4-DACH)] complex was quantitatively bound after 24 h. This result indicates that the rate of binding of [$PtCl_2$(*cis*-1,4-DACH)] to natural double-helical DNA is higher than that of cisplatin or *trans*-dimminedichloridoplatinum(II) (transplatin) ($t_{50\%}$ = ca. 120 min [61]).

The binding experiments of the present work indicate that the modification reactions resulted in the irreversible coordination of [$PtCl_2$(*cis*-1,4-DACH)] to polymeric double-helical DNA, which also facilitates sample analysis. Hence, it is possible to prepare easily and precisely the samples of DNA modified by the platinum complex at a preselected value of r_b. The samples of DNA modified by [$PtCl_2$(*cis*-1,4-DACH)] or cisplatin and analyzed further by biophysical or biochemical methods were prepared in 10 mM $NaClO_4$ at 37 °C. If not stated otherwise, after 24 h reaction of DNA with the complex, the samples were precipitated in ethanol, dissolved in the medium necessary for a particular analysis and the r_b value in an aliquot of this sample was checked by FAAS. In this way, the analyses described in the present paper were performed in the absence of unbound (free) platinum complex.

3.4.2. Replication mapping of platinum–DNA adducts

This procedure involved the extension by VentR(exo$^-$) DNA polymerase at the 3′-end of the primer up to the metal adduct on the template strand of pSP73 DNA. The products of the synthesis were then examined on DNA sequencing gels, and the sequence specificity of the platinum adduct formation was determined to

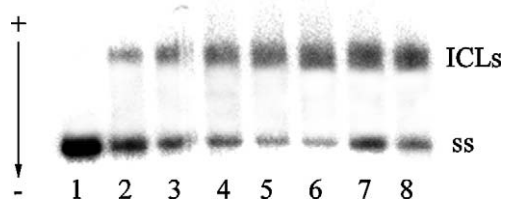

Fig. 3. DNA interstrand cross-linking. The formation of interstrand CLs by [$PtCl_2$(*cis*-1,4-DACH)] in linear pSP73KB plasmid DNA. Autoradiogram of a denaturing 1% agarose gels of linearized DNA which was 3′-end labeled; the interstrand cross-linked DNA appears as the top bands migrating on the gels more slowly than the single-stranded DNA (contained in the bottom bands). Lanes: 1–6, 1,4-DACH, r_b = 0, 0.001, 0.0015, 0.002, 0.0025, 0.003, respectively; lanes 7, 8, cisplatin, r_b = 0.0015 and 0.0025, respectively.

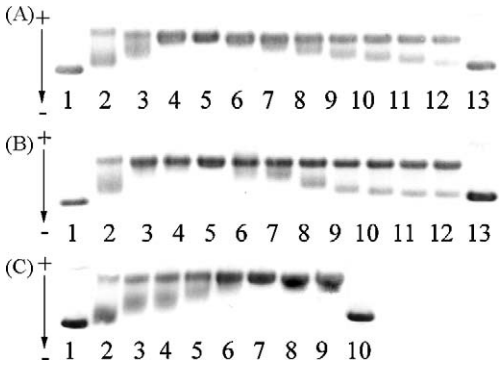

Fig. 4. DNA unwinding. Unwinding of negatively supercoiled pSP73KB plasmid DNA by cisplatin (A) and [$PtCl_2$(*cis*-1,4-DACH)] (B and C). The top bands in each panel correspond to the form of nicked plasmid and the bottom bands to the closed, negatively supercoiled plasmid. (A) Cisplatin. Lanes: 1 and 13—control, nonmodified DNA, 2–12, r_b = 0.02, 0.03, 0.04, 0.05, 0.06, 0.07, 0.08, 0.09, 0.10, 0.11, 0.12, respectively. (B) [$PtCl_2$(*cis*-1,4-DACH)]. Lanes: 1 and 13—control, nonmodified DNA, 2–12, r_b = 0.02, 0.03, 0.04, 0.05, 0.06, 0.07, 0.08, 0.09, 0.10, 0.11, 0.12, respectively. (C) [$PtCl_2$(*cis*-1,4-DACH)]. Lanes: 1 and 10—control, nonmodified DNA, 2–9, r_b = 0.020, 0.030, 0.035, 0.040, 0.045, 0.050, 0.055, 0.060, respectively.

the exact base pair. *In vitro* DNA synthesis on DNA templates containing the adducts of [$PtCl_2$(*cis*-1,4-DACH)] generated a population of DNA fragments, indicating that the adducts of this complex effectively terminate DNA synthesis (Fig. 2A, lane 1,4-DACH). Sequence analysis of the termination sites produced by [$PtCl_2$(*cis*-1,4-DACH)] suggests a strong preference of DNA binding to dG sites and in some extent also to dA sites (Fig. 2B), i.e. this platinum complex exhibited a sequence preference identical to that of cisplatin and different from that of ineffective transplatin (compare lanes 1,4-DACH with cisPt and transPt in Fig. 2A).

3.4.3. Interstrand cross-linking

Bifunctional platinum compounds, which coordinate base residues in DNA, form various types of interstrand and intrastrand CLs. Considerable evidence suggests that the antitumor efficacy of bifunctional platinum compounds is the result of the formation of these lesions, but their relative efficacy remains unknown. Therefore, we have decided to quantitate the interstrand cross-linking efficiency of [$PtCl_2$(*cis*-1,4-DACH)] in linearized pSP73KB plasmid. This plasmid DNA was linearized by EcoRI (EcoRI cuts only once within pSP73KB plasmid) and globally modified by [$PtCl_2$(*cis*-1,4-DACH)], cisplatin or transplatin. The samples were analyzed for the interstrand CLs by agarose gel electrophoresis under denaturing conditions [35]. Upon electrophoresis, 3′-end labeled strands of linearized pSP73 plasmid containing no interstrand CLs migrate as a 2456-base single strand, whereas the interstrand cross-linked strands migrate more slowly as a higher molecular mass species (Fig. 3). The experiments were carried out with DNA samples that were modified by the platinum complex at various r_b values. The intensity of the more slowly migrating band increased with the growing level of the platination. The radioactivity associated with the individual bands in each lane was measured to obtain estimates of the fraction of non-cross-linked or cross-linked DNA under each condition. The DNA interstrand cross-linking efficiency of the [$PtCl_2$(*cis*-1,4-DACH)] was 6 ± 1% (Table 1). It implies that interstrand CLs represent only minor portion of the adducts formed in DNA by [$PtCl_2$(*cis*1,4-DACH)].

3.4.4. Unwinding of negatively supercoiled DNA

Electrophoresis in native agarose gel was used to determine the unwinding induced in negatively supercoiled pSP73KB plasmid by monitoring the degree of supercoiling [38] (Fig. 4). A compound that unwinds the DNA duplex reduces the number of supercoils in closed circular DNA so that their number decreases. This decrease upon binding of unwinding agents causes a decrease in the rate of migration through agarose gel, which makes it possible to observe and quantify the mean value of unwinding per one adduct. Fig. 4 shows electrophoresis gels from the experiment in which variable amounts of cisplatin or [$PtCl_2$(*cis*-1,4-DACH)] have been bound to a mixture of relaxed and negatively supercoiled pSP73KB DNA. The mean unwinding angle is given by $\Phi = -18\sigma/r_b(c)$, where σ is the superhelical density and $r_b(c)$ is the value of r_b at which the supercoiled and nicked forms co-migrate [38]. Under the present experimental conditions, σ was calculated to be −0.0505 on the basis of the data of cisplatin for which the $r_b(c)$ was determined in this study and $\Phi = 13^\circ$ was assumed. Using this approach, the DNA unwinding angle of $15 \pm 2^\circ$ was determined.

3.4.5. Chemical probes of DNA conformation

The replication mapping experiments demonstrated that [$PtCl_2$(*cis*-1,4-DACH)] binds to DNA at the same sites as cisplatin, which preferentially forms 1,2-intrastrand CLs between two neighboring guanine residues. In addition, [$PtCl_2$(*cis*-1,4-DACH)] forms on DNA minor interstrand CLs at the same frequency as cisplatin. Thus, it is reasonable to assume that 1,2-GG intrastrand CLs are also the major lesions formed on DNA by [$PtCl_2$(*cis*-1,4-DACH)]. Therefore, in the next experiments, we have focused on the characterization of the DNA perturbations induced in DNA by 1,2-GG intrastrand CL of [$PtCl_2$(*cis*-1,4-DACH)].

To further characterize the conformational distortion induced in DNA by the 1,2-GG intrastrand CLs of [$PtCl_2$(*cis*-1,4-DACH)], the 22-bp oligonucleotide duplex [TGGT(22) shown in Fig. S1A] containing the single, site-specific 1,2-GG intrastrand CL of [$PtCl_2$(*cis*-1,4-DACH)] (and for comparative purposes also the CL of cisplatin) was treated with several chemical agents that are used as tools for monitoring the existence of conformations other than canonical B-DNA. These agents include $KMnO_4$, DEPC, and bromine. These probes react, under the conditions used, with base residues in single-stranded DNA and distorted double-stranded DNA, but not with the base residues in intact, double-stranded DNA [27,39–41]. For this analysis, we used exactly the same methodology as in our recent studies dealing with DNA adducts of various antitumor platinum drugs. Thus, the details of this experiment can be found in those articles and representative gels showing piperidine-induced specific strand cleavage at $KMnO_4$-modified, KBr/$KHSO_5$-modified and DEPC-modified bases in the 22-bp duplex unplatinated or containing single, interstrand CL of [$PtCl_2$(*cis*-1,4-DACH)] or cisplatin are demonstrated in Fig. S1A. The results are schematically summarized in Fig. S1B and Table 1. The pattern and degree of reactivity toward the

chemical probes found for the 1,2-GG intrastrand CLs formed by [$PtCl_2$(*cis*-1,4-DACH)] and cisplatin were identical.

3.4.6. DNA unwinding and bending by 1,2-GG intrastrand cross-link of [$PtCl_2$(*cis*-1,4-DACH)]

Among the alterations of secondary and tertiary structure of DNA, the role of intrinsic bending of DNA is increasingly recognized as of potential importance in regulating replication, transcription and repair functions through specific DNA–protein interactions. For DNA adducts of cisplatin, the structural details responsible for bending and subsequent protein recognition have recently been elucidated [62,63]. Given the recent advances in our understanding of the structural basis for the bending of DNA caused by 1,2-GG intrastrand CL of cisplatin, it is of considerable interest to examine how the same adduct of [$PtCl_2$(*cis*-1,4-DACH)] affects conformational properties of DNA such as unwinding and bending. In this work we further performed studies on the bending and unwinding induced by the single, site-specific 1,2-GG intrastrand CL of [$PtCl_2$(*cis*-1,4-DACH)] formed in oligodeoxyribonucleotide duplexes.

As in the previous studies [19,64], we used electrophoretic retardation as a quantitative measure of the extent of planar curvature to analyze bending and unwinding induced by the single, site-specific 1,2-GG intrastrand CL formed by [$PtCl_2$(*cis*-1,4-DACH)] in the sequence TGGT. The oligodeoxyribonucleotide duplexes TGGT (19–23) used for DNA bending and unwinding studies were 19–23-bp long (for their sequence, see Fig. S2A). The ligation products of these unplatinated or [Pt(*cis*-1,4-DACH)]-containing duplexes were analyzed on native PAA electrophoresis gel. Experimental details of these studies are given in our recent reports [19,64]. A representative gel and its analysis showing the mobility of the ligation products of 19–23-bp duplexes containing single, site-specific 1,2-GG intrastrand CL of [$PtCl_2$(*cis*-1,4-DACH)] at the central sequence TGGT in a PAA gel is demonstrated in the Supplementary Material (Fig. S2B). The results are summarized in Table 1. The DNA bending toward the major groove of $33 \pm 1^\circ$ and unwinding $19 \pm 2^\circ$ due to the single, site-specific 1,2-GG intrastrand CL formed by [$PtCl_2$(*cis*-1,4-DACH)] were found. The direction of the bend was determined using the 33-bp duplexes, which also contained, besides the single 1,2-GG intrastrand CL formed by [$PtCl_2$(*cis*-1,4-DACH)], the $(A\text{-}T)_5$ tract located "in phase" from the CL (the cross-linked base pair and the center of the A tract were separated by 11 bp), in the same way as in our recent articles [65–67]. Also produced in ligations of monomers investigated in this work were separate bands arising from small DNA circles that migrate close to the top of the gel (see the bands marked by asterisk in Fig. S2B). The highest tendency to yield DNA circles was observed for the 22-bp multimers confirming a close match between the 22-bp sequence repeats and the helix screw [68,69]. Taken together, the major 1,2-GG intrastrand CL bends DNA in the same way as the same adduct of cisplatin whereas this CL formed by [$PtCl_2$(*cis*-1,4-DACH)] in the sequence TGGT unwinds DNA somewhat more.

3.5. Inhibition of DNA polymerization

It has been demonstrated that DNA modifications by various platinum complexes have significant effects on processivity of a number of prokaryotic, eukaryotic, and viral DNA polymerases [45,70–75]. Interestingly, with DNA templates containing site-specifically placed adducts of various platinum compounds, a number of prokaryotic and eukaryotic DNA polymerases were blocked but could also traverse through platinum adducts, depending on their character and conformational alterations

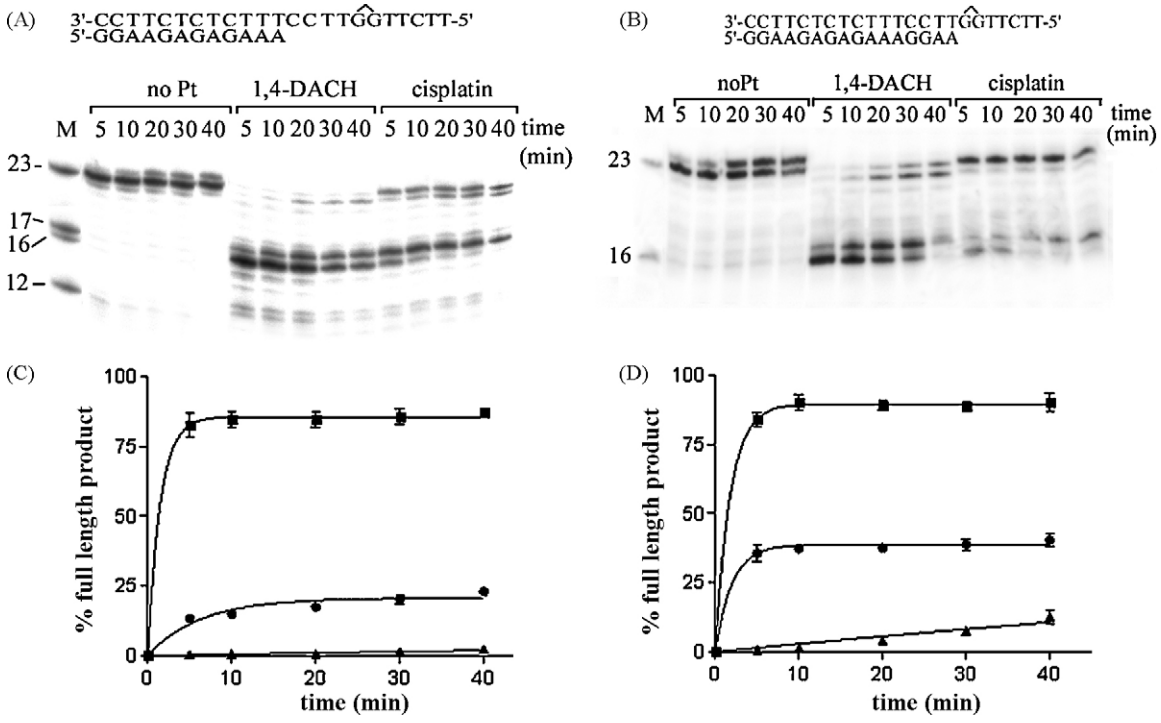

Fig. 5. Primer extension activity of KF^-. The experiments were conducted using the 12-mer/23-mer ("running start" experiment) (A) or 16-mer/23-mer ("standing start" experiment) (B) primer-template duplexes for the times indicated. These duplexes were unplatinated or contained single 1,2-intrastrand CL formed at the neighboring guanine residues in the TGGT sequence by [$PtCl_2$(*cis*-1,4-DACH)] or cisplatin. The nucleotide sequences of the templates and the primers are shown above the gels. See the text for details. (A) The strong band marked 12 corresponds to the 12-mer primer; the strong pause sites opposite one base before and the platinated 3′ guanine are marked 16 and 17, respectively; the bands marked 23 correspond to the full-length products. (B) The strong band marked 16 corresponds to the 16-mer primer; the bands marked 23 correspond to the full-length products. (C and D) The time dependence of the inhibition of DNA synthesis on undamaged (control) template (squares), DNA containing the CL of [$PtCl_2$(*cis*-1,4-DACH)] (triangles) or cisplatin (circles); (C) "running start" experiment, (D) "standing start" experiment. Data are means (±SEM) from three different experiments with two independent template preparations.

induced in DNA. It is therefore of great interest to examine whether DNA polymerases, processing DNA substrates containing 1,2-GG intrastrand CL of [$PtCl_2$(*cis*-1,4-DACH)] and cisplatin could reveal potential differences in alterations imposed on DNA by CLs of these two Pt^{II} complexes which differ in the nonleaving amine ligands.

We investigated in the present work DNA polymerization using the templates site-specifically modified by the 1,2-GG intrastrand CL of [$PtCl_2$(*cis*-1,4-DACH)] or cisplatin by KF^- as a model and well characterized enzyme frequently used in the studies aimed at understanding the processes in which nucleic acid polymerases take part.

We constructed, for the first series of experiments (''running start'' [48]), the 12-mer/23-mer primer-template duplexes (Fig. 5A) unplatinated or containing single 1,2-GG intrastrand CL of the cis-Pt^{II} complex. The first 12 nucleotides on the 3′ terminus of the 23-mer template strand were complementary to the nucleotides of the 12-mer primer so that the 3′ guanine involved in the CL on the template strand was located at its 17th position from the 3′ terminus (Fig. 5A). After annealing the 12-nucleotide primer to the 3′ terminus of the unplatinated or platinated template strand (positioning the 3′-end of the primer five bases before the adduct in the template strand), we examined DNA polymerization through the 1,2-GG intrastrand CL of [$PtCl_2$(*cis*-1,4-DACH)] or cisplatin by KF^- in the presence of all four dNTPs. The reaction was stopped at various time intervals, and the products were analyzed using a sequencing gel (Fig. 5A). Polymerization by KF^- using the 12-mer/23-mer primer-templates containing the 1,2-GG intrastrand CL of [$PtCl_2$(*cis*-1,4-DACH)] or cisplatin in the presence of all four dNTPs proceeded rapidly up to the nucleotide opposite the base immediately downstream from the CL and the 3′ guanine involved in the CL, such that the 16- and 17-nucleotide intermediate products accumulated to a significant extent (shown in Fig. 5A). There was only a slight accumulation of longer DNA intermediates and more extensive accumulation of full length (23-nucleotide) products in particular using the templates containing the CL of cisplatin, whereas no full length products and only a very slight accumulation of longer intermediate products were seen with the template containing the CL of [$PtCl_2$(*cis*-1,4-DACH)]. No intermediates, but only full length products were seen with the 23-mer unplatinated control template (shown in Fig. 5A).

For the other series of experiments (''standing start'' [48]), we constructed the 16-mer/23-mer primer-template duplexes (Fig. 5B) unplatinated or containing 1,2-GG intrastrand CL of the cis-Pt^{II} complex. The first 16 nucleotides on the 3′ terminus of the 23-mer template strand were complementary to the nucleotides of the 16-mer primer (Fig. 5B). Thus, after annealing the 16-nucleotide primer to the 3′ terminus of the unplatinated or platinated template strand (positioning the 3′-end of the primer only one base before the adduct in the template strand), we examined DNA polymerization through the 1,2-GG intrastrand CL of [$PtCl_2$(*cis*-1,4-DACH)] or cisplatin by KF^- in the presence of all four dNTPs in the same way as in the case of the ''running start'' experiment (Fig. 5A). Polymerization by KF^- using the 16-mer/23-mer primer-template containing the 1,2-GG intrastrand CL of cisplatin in the presence of all four dNTPs proceeded rapidly only up to the 3′ guanine involved in the CL (so that only one nucleotide was added), such that the 17-nucleotide intermediate products accumulated to some extent (shown in Fig. 5B). There was only a very slight accumulation of larger DNA intermediates, but a relatively large accumulation of full length products. In contrast, the 1,2-GG intrastrand CLs of [$PtCl_2$(*cis*-1,4-DACH)] inhibited polymerization by KF^- markedly more efficiently in this ''standing start'' experiment as well. The 17-nucleotide intermediate products accumulated to a markedly larger extent with only a slight accumulation of 22-nucleotide intermediates or 23-nucleotide full length products. No intermediates and only full length products were seen with the 23-mer unplatinated control template in the ''standing start'' experiment as well (shown in Fig. 5B).

Next we characterized nucleotide incorporation opposite the 1st (3′) platinated G involved in the 1,2-GG intrastrand CL of cisplatin or [$PtCl_2$(*cis*-1,4-DACH)] [using the 16-mer/23-mer primer-template duplexes (Fig. S3) having a target template base, 1st (3′) platinated G involved in the 1,2-GG intrastrand CL, adjacent to a primer 3′-terminus] by KF^- more quantitatively. Thus, the kinetic parameters of dCTP insertion were measured in ''standing start'' experiment on templates containing single, site-specific 1,2-GG intrastrand CL of [$PtCl_2$(*cis*-1,4-DACH)] or cisplatin and undamaged templates. The kinetics of insertion of a single dCTP opposite the complementary 1st (3′) platinated G involved in the CL to 3′-primer termini situated across the platinated G were determined as a function of dCTP concentration under steady-state conditions. For purposes of comparison, the kinetic parameters of dCTP insertion opposite this G residue contained in the unplatinated template were measured as well. From the kinetics of dCTP incorporation, the steady-state apparent K_m and V_{max} values for the incoming dCTP opposite the template platinated 3′ G in the 1,2-GG-intrastrand CL of [$PtCl_2$(*cis*-1,4-DACH)] or cisplatin or this G residue contained in the unplatinated template were obtained from the curves fitted to the Michaelis–Menten equation in the same way as in the previous papers (see e.g. Refs. [47–50]). The patterns of deoxyribonucleotide incorporation by KF^- opposite the 1st (3′) G residue contained in the 1,2-GG-intrastrand CL of [$PtCl_2$(*cis*-1,4-DACH)] or cisplatin are shown in Fig. S3A and B, respectively. The K_m and V_{max} parameters were determined and used to calculate the percentage of dCTP incorporated opposite the platinated G residues (Table 2).

As indicated by the V_{max}/K_m values, KF^- inserted dCTP opposite the 1st (3′) G residue contained in the 1,2-GG-intrastrand CL of cisplatin about 200-fold less efficiently than opposite this G which

Table 2
Kinetics of incorporation of dCTP opposite the 1st (3′) platinated G in the 1,2-GG intrastrand CL by KF^-.

DNA substrate	K_m (μM)	V_{max} (%/min)	V_{max}/K_m	Relative efficiency[a]
5′——A 3′——TGGT——	0.0031 ± 0.0007	18.4 ± 0.7	5936	1
5′----A 3′----TGGT---- cisplatin	0.51 ± 0.08	16.3 ± 1.2	32	0.0054
5′----A 3′----TGGT---- Pt(*cis*-1,4-DACH)	9.1 ± 0.9	16.7 ± 0.5	1.8	0.0003

[a] Compares the efficiency of the dCTP insertion opposite the template 1st (3′) platinated G to the efficiency of the dCTP insertion opposite this G which was unplatinated.

was contained in the unplatinated template. In contrast, incorporation of dCTP by KF^- opposite the 1st (3′) G in the same CL of [$PtCl_2$(*cis*-1,4-DACH)] was even more than 3000-fold less efficient than opposite this G which was contained in the unplatinated template. The substantially lower efficiency of dCTP incorporation opposite the 1st (3′) G contained in the 1,2-GG-intrastrand CL of the Pt^{II} complexes resulted from a 164 and 2935-fold increase in the K_m (Table 2).

The results of experiments demonstrating the effects of major DNA adducts of [$PtCl_2$(*cis*-1,4-DACH)] and cisplatin on DNA polymerization indicate that the character of these adducts and alterations induced in DNA by these adducts were distinctly different so that the replacement of nonleaving ammine groups in cisplatin by a large-ring *cis*-1,4-DACH carrier ligand led to DNA adducts that could potentially impede elongation of DNA markedly more effectively.

3.6. DNA repair synthesis by human cell extract

DNA repair efficiency in pSP73 plasmid (2464 bp) globally modified by [$PtCl_2$(*cis*-1,4-DACH)] and cisplatin was tested using CFE of repair proficient HeLa cells. Repair activity was monitored by measurement of the amount of incorporated radiolabelled nucleotide. The incorporation of radioactive material was corrected for the relative DNA content in each band. As illustrated in Fig. 6, damage-induced DNA repair synthesis detected in the plasmid modified by [$PtCl_2$(*cis*-1,4-DACH)] was approximately 85% of that found for the cisplatin at the same level of modification.

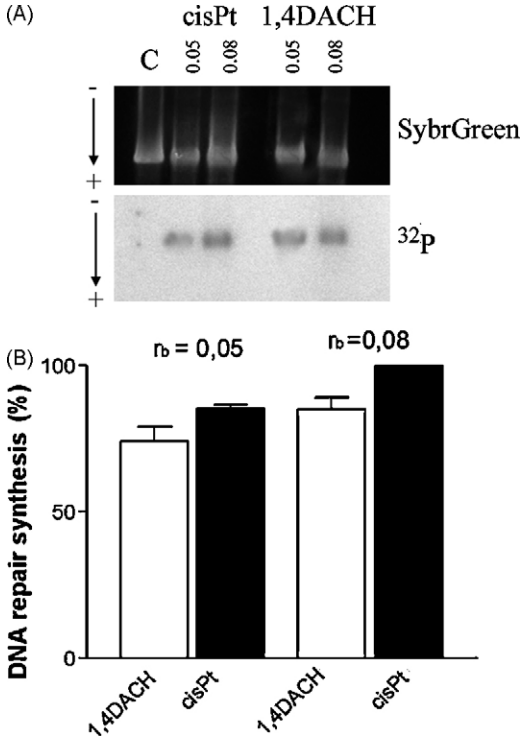

Fig. 6. *In vitro* DNA repair synthesis assay of the extract prepared from the repair-proficient HeLa cell line. Repair synthesis used as substrates pSP73 plasmid nonmodifed (lane C) or modified at r_b = 0.05 or 0.08 by cisplatin (lanes cisPt 0.05 and cis Pt 0.08, respectively) or by [$PtCl_2$(*cis*-1,4-DACH)] (lanes 1,4DACH 0.05 and 1,4DACH 0.08, respectively). (A) Results of a typical experiment. The top panel is a photograph of the SybrGreen stained gel and the bottom panel is the autoradiogram of the gel showing incorporation of [α-^{32}P]dCTP. (B) Incorporation of dCTP into platinated plasmids. For all quantifications representing mean values of the two independent experiments, incorporation of radioactive material is corrected for the relative DNA content in each band. Bars indicate SEM.

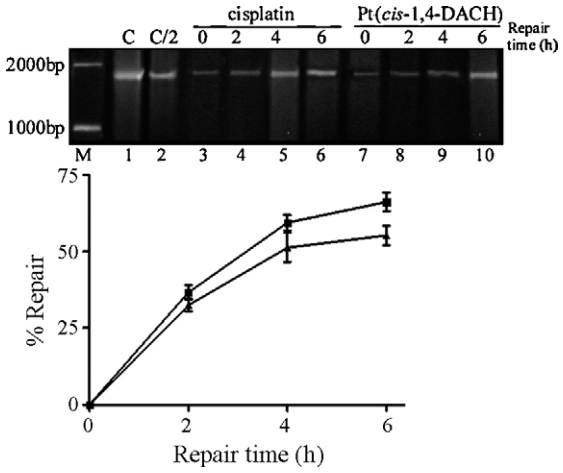

Fig. 7. Repair of [$PtCl_2$(*cis*-1,4-DACH)]- and cisplatin-induced DNA lesions in the *DHRF* gene. (A) A representative image of amplification products resolved on 1% agarose gel. Lanes: M, 1000 and 2000 bp markers; 1, the product of amplification of undamaged template (150 ng DNA isolated from untreated cells); 2, the product obtained by amplification of half the amount of undamaged template DNA (75 ng); 3–6, products of amplification of 150 ng DNA isolated from cells treated with cisplatin; 7–10, products of amplification of 150 ng DNA isolated from cells treated with [$PtCl_2$(*cis*-1,4-DACH)]. (B) Quantitation of [$PtCl_2$(*cis*-1,4-DACH)]- (▲) or cisplatin-induced (■) adducts removal from the *DHRF* gene plotted as a function of repair time. Data are means (±SEM) from three independent experiments. For other details, see the text.

3.7. Inhibition of repair in human ovarian A2780 cells

To further characterize the ability of cellular repair system to remove [$PtCl_2$(*cis*-1,4-DACH)]-induced DNA lesions, the repair of platinum adducts was directly examined in living cells as well. The quantitative PCR assay was used to investigate the removal of [$PtCl_2$(*cis*-1,4-DACH)]-induced lesions in the *DHFR* gene. A2780 cells were incubated with [$PtCl_2$(*cis*-1,4-DACH)] or cisplatin to induce damage, followed by treatment with thiourea (to prevent the slow conversion of monoadducts to CLs) before the cells were allowed to repair the damage. The DNA was then isolated and analyzed for the presence of platinum lesions in the *DHFR* gene. In A2780 cells, as seen in Fig. 7, lesions induced by [$PtCl_2$(*cis*-1,4-DACH)] were repaired rapidly, with 55 ± 5% of lesions removed within 6 h. Similar results were obtained for the repair of cisplatin-induced lesions, 64 ± 5% of total lesions were repaired in 6 h. Hence, the results of this experiment confirmed that also in cells [$PtCl_2$(*cis*-1,4-DACH)] adducts are removed from DNA with only slightly slower repair kinetics than DNA adducts of cisplatin, in agreement with the *in vitro* results obtained using CFEs.

4. Discussion

[$PtCl_2$(*cis*-1,4-DACH)] proved to be quite toxic to the tumor cells, with IC_{50} values that were lower than those observed for cisplatin [20] (Table 1). Interestingly, the cytotoxicity of [$PtCl_2$(*cis*-1,4-DACH)] in the cisplatin-resistant line A2780cisR is also characterized by a lower resistance factor (Table 1).

The origin of the improved pharmacological effects of [$PtCl_2$(*cis*-1,4-DACH)] may be multifactorial. The major pharmacological factors affecting platinum drug cytotoxicity are cellular uptake and efflux; structure and frequency of target (DNA) adducts, including their intracellular processing; and metabolic deactivation by sulfur nucleophiles [16,76]. All these factors combine to affect signaling pathways, leading to apoptosis or necrosis of tumor cells.

The present study reveals that the cellular uptake of [$PtCl_2$(*cis*-1,4-DACH)] is considerably greater than that of cisplatin (Table 1).

Structure-activity studies indicate that organic functionalities on nonleaving groups of Pt^{II} complexes, such as 1,2-DACH [77] or diammine(pyridine) [78] coordinated to platinum positively correlate with enhanced cellular uptake mediated by the human organic cation transporters in comparison with purely inorganic cisplatin [77]. Thus, the observation that the cellular uptake of [$PtCl_2$(*cis*-1,4-DACH)] is greater than that of cisplatin is consistent with an organic character of the nonleaving ligand of the [$PtCl_2$(*cis*-1,4-DACH)] complex. Hence, the results confirm the enhanced uptake of [$PtCl_2$(*cis*-1,4-DACH)] so that at least part of the increased cytotoxicity of this 1,4-DACH complex over cisplatin seems to be attributable to an increased intracellular accumulation.

The results of the present work also demonstrate that [$PtCl_2$(*cis*-1,4-DACH)] reacts with GSH and MT-2 with a rate higher or similar to that of parent cisplatin (Table 1). In contrast, this 1,4-DACH compound is pronouncedly more potent also in the tumor cell line A2780cisR resistant to cisplatin (Table 1), which is known to be resistant also through elevated levels of reduced GSH [79]. Hence, the unfavorable deactivation of Pt^{II} compounds by GSH does not seem to be a strong determinant of cytotoxic effects of [$PtCl_2$(*cis*-1,4-DACH)].

The adducts of conventional cisplatin and its analogues distort DNA conformation [15,80], inhibit replication and transcription (but they are also bypassed by DNA or RNA polymerases) [17,81], and trigger apoptosis or necrosis [82]. In addition, cisplatin adducts are removed from DNA mainly by nucleotide excision repair system [15,80] and are also recognized by several proteins [83]. In broad terms, we have demonstrated that the DNA binding mode of [$PtCl_2$(*cis*-1,4-DACH)], including sequence preference, type of the major adducts, and resulting conformational alterations, is not very different from that of cisplatin (Table 1). In contrast, there are differences in some factors associated with the DNA binding mode, which may be relevant to different biological effects of [$PtCl_2$(*cis*-1,4-DACH)] and cisplatin. The major adducts of [$PtCl_2$(*cis*-1,4-DACH)] are removed from DNA by DNA repair systems present in CFEs and in living cells as well with a slightly lower efficiency than the adducts of cisplatin (Fig. 6). Hence, it cannot be excluded that they may persist somewhat longer on DNA than the adducts of cisplatin, which may potentiate probably only partially antitumor effects of [$PtCl_2$(*cis*-1,4-DACH)].

Most interestingly, the 1,2-GG intrastrand CLs of [$PtCl_2$(*cis*-1,4-DACH)] inhibit DNA polymerization more efficiently than the same adducts of cisplatin (Fig. 5 and Fig. S3, Tables 1 and 2) so that they can also be bypassed by DNA polymerases with greater difficulty. Numerous studies have indicated that the level of DNA adduct tolerance, which has been correlated with the increased ability of DNA polymerases to replicate DNA past platinum adducts, inversely correlates with sensitivity to platinum drugs [84,85]. In other words, the sensitivity of tumor cells to platinum drugs can be enhanced as a consequence of a lowered adduct tolerance mediated by reduced ability of DNA polymerases to replicate past platinum adducts. We find in the present work that major DNA adducts of [$PtCl_2$(*cis*-1,4-DACH)] impede elongation of DNA by a model prokaryotic DNA polymerase KF^- to a markedly greater extent than those of cisplatin (Fig. 5 and Fig. S3, Tables 1 and 2). Since there is a high degree of structural and sequence conservation of the domains among eukaryotic, prokaryotic, and viral polymerases [86] insights gleaned from studies of the KF^- should be also applicable to other DNA polymerases [87–89]. Hence, the repercussion of stronger inhibition of DNA polymerization by the 1,2-intrastrand CL of [$PtCl_2$(*cis*-1,4-DACH)] in comparison with the major adduct of cisplatin adds a new dimension to the impact of the replacement of the ammonia groups in cisplatin by *cis*-1,4-DACH ligand on biological processes, possibly including replication or DNA repair.

A gently tuned catalytically active structure of the ternary DNA polymerase·primer/template DNA·incoming dNTP complex is a prerequisite for correct course of the DNA polymerization reaction. In regard to the different effects of DNA adducts of [$PtCl_2$(*cis*-1,4-DACH)] and cisplatin on the DNA polymerization reaction (Fig. 5 and Fig. S3), the formation of this ternary complex can be disturbed by (i) different conformational distortions imposed on the template DNA by the two Pt^{II} complexes or (ii) steric clashes between the bulkier 1,4-DACH ligand of the DNA adduct and other components of the ternary complex, which do not occur in the case of considerably less bulky nonleaving ammonia ligands of the DNA adduct of cisplatin. As the conformational distortions induced in DNA by DNA adducts of [$PtCl_2$(*cis*-1,4-DACH)] and cisplatin are similar (Table 1), the bulk size appears to be a major factor responsible for the markedly lowered tolerance of DNA adducts of [$PtCl_2$(*cis*-1,4-DACH)].

The inhibition of DNA polymerization by Pt–DNA adducts appears to be one of the most pronounced effects observed in the present work that could be responsible for markedly different effects of DNA adducts of [$PtCl_2$(*cis*-1,4-DACH)] and cisplatin (Tables 1 and 2). The studies demonstrating lowered ability of DNA polymerases to replicate DNA past platinum adducts were performed in the present work using one of the most intensively studied DNA polymerases, a model prokaryotic DNA polymerase KF^- of A-family of DNA polymerases, which has served as a prototype for studying DNA polymerase mechanisms [90]. Nevertheless, a more detailed study of DNA polymerization across and beyond the adducts of [$PtCl_2$(*cis*-1,4-DACH)] and cisplatin using eukaryotic translesion DNA polymerases of Y-family are warranted. These studies are in progress in our laboratory in Brno and results of these detailed studies will be published in a separate report.

The cytotoxicity is the result of many events, beginning with the cell accumulation and proceeding through detoxification by thiols, DNA modification, and cellular responses to the DNA damage. It is not a simple task to reveal all aspects of the mechanism underlying antitumor effects of platinum complexes, and it is apparently incorrect to attribute cytotoxicity to their single property. Further studies are therefore warranted to reveal a relative contribution of all potential factors contributing to the potency of [$PtCl_2$(*cis*-1,4-DACH)] in various types of cancer cells.

Acknowledgements

This research was supported by the Ministry of Education of the CR (MSMT LC06030, 6198959216, ME08017, OC08003, OC09018), the Academy of Sciences of the Czech Republic (Grants 1QS500040581, KAN200200651, M200040901, AV0Z50040507 and AV0Z50040702), the Grant Agency of the Academy of Sciences of the CR (IAA400040803), the Grant Agency of the CR (301/09/H004), the University of Bari and the M.I.U.R., Italy. J.K. is the international research scholar of the Howard Hughes Medical Institute. The authors also acknowledge that their participation in the EU COST Action D39 enabled them to exchange regularly the most recent ideas in the field of anticancer metallodrugs with several European colleagues.

Appendix A. Supplementary data

Supplementary data associated with this article can be found, in the online version, at doi:10.1016/j.bcp.2009.09.019.

References

[1] Kelland L. The resurgence of platinum-based cancer chemotherapy. Nat Rev Cancer 2007;7:573–84.

[2] Ronconi L, Sadler PJ. Using coordination chemistry to design new medicines. Coord Chem Rev 2007;251:1633–48.
[3] Massey A, Offman J, Macpherson P, Karran P. DNA mismatch repair and acquired cisplatin resistance in *E. coli* and human ovarian carcinoma cells. DNA Repair 2003;2:73–89.
[4] Stewart DJ. Mechanisms of resistance to cisplatin and carboplatin. Crit Rev Oncol Hematol 2007;63:12–31.
[5] Kelland LR, Sharp SY, ONeill CF, Raynaud FI, Beale PJ, Judson IR. Mini-review: discovery and development of platinum complexes designed to circumvent cisplatin resistance. J Inorg Biochem 1999;77:111–5.
[6] LaPensee EW, Schwemberger SJ, LaPensee CR, Bahassi EM, Afton SE, Ben-Jonathan N. Prolactin confers resistance against cisplatin in breast cancer cells by activating glutathione-S-transferase. Carcinogenesis 2009;30:1298–304.
[7] McPherson RAC, Galettis PT, de Souza PL. Enhancement of the activity of phenoxodiol by cisplatin in prostate cancer cells. Br J Cancer 2009;100:649–55.
[8] Harder HC, Rosenberg B. Inhibitory effects of anti-tumor platinum compounds on DNA, RNA and protein synthesis in mammalian cells in vitro. Int J Cancer 1970;6:207–16.
[9] Howle JA, Gale GR. cis-Dichlorodiammineplatinum(II): persistent and selective inhibition of DNA synthesis in vivo. Biochem Pharmacol 1970;19:2757–62.
[10] Johnson NP, Butour J-L, Villani G, Wimmer FL, Defais M, Pierson V, et al. Metal antitumor compounds: the mechanism of action of platinum complexes. Prog Clin Biochem Med 1989;10:1–24.
[11] Cullen KJ, Yang ZJ, Schumaker L, Guo ZM. Mitochondria as a critical target of the chemotheraputic agent cisplatin in head and neck cancer. J Bioenerg Biomembr 2007;39:43–50.
[12] Rebillard A, Tekpli X, Meurette O, Sergent O, LeMoigne-Muller G, Vernhet L, et al. Cisplatin-induced apoptosis involves membrane fluidification via inhibition of NHE1 in human colon cancer cells. Cancer Res 2007;67:7865–74.
[13] Ragunathan N, Dairou J, Pluvinage B, Martins M, Petit E, Janel N, et al. Identification of the xenobiotic-metabolizing enzyme arylamine N-acetyltransferase 1 as a new target of cisplatin in breast cancer cells: molecular and cellular mechanisms of inhibition. Mol Pharmacol 2008;73:1761–8.
[14] Jamieson ER, Lippard SJ. Structure, recognition, and processing of cisplatin–DNA adducts. Chem Rev 1999;99:2467–98.
[15] Brabec V. DNA modifications by antitumor platinum and ruthenium compounds: their recognition and repair. Prog Nucleic Acid Res Mol Biol 2002;71:1–68.
[16] Brabec V, Kasparkova J. Modifications of DNA by platinum complexes: relation to resistance of tumors to platinum antitumor drugs. Drug Resist Updates 2005;8:131–46.
[17] Jung Y, Lippard SJ. Direct cellular responses to platinum-induced DNA damage. Chem Rev 2007;107:1387–407.
[18] Kasparkova J, Vojtiskova M, Natile G, Brabec V. Unique properties of DNA interstrand cross-links of antitumor oxaliplatin and the effect of chirality of the carrier ligand. Chem Eur J 2008;14:1330–41.
[19] Malina J, Novakova O, Vojtiskova M, Natile G, Brabec V. Conformation of DNA GG intrastrand cross-link of antitumor oxaliplatin and its enantiomeric analog. Biophys J 2007;93:3950–62.
[20] Hoeschele JD, Showalter HDH, Kraker AJ, Elliott WL, Roberts BJ, Kampf JW. Synthesis, structural characterization, and antitumor properties of a novel class of large-ring platinum(II) chelate complexes incorporating the cis-1,4-diaminocyclohexane ligand in a unique locked boat conformation. J Med Chem 1994;37:2630–6.
[21] Knox RJ, Friedlos F, Lydall DA, Roberts JJ. Mechanism of cytotoxicity of anticancer platinum drugs: evidence that cis-diamminedichloroplatinum(II) and cis-diammine(1,1,-cyclobutanedicarboxylato)platinum(II) differ only in the kinetics of their interaction with DNA. Cancer Res 1986;46:1972–9.
[22] Shamsuddin S, Santillan CC, Stark JL, Whitmire KH, Siddik ZH, Khokhar AR. Synthesis, characterization, and antitumor activity of new platinum(IV) trans-carboxylate complexes: crystal structure of [Pt(cis-1,4-DACH)trans-(acetate)$_2$Cl$_2$]. J Inorg Biochem 1998;71:29–35.
[23] Shamsuddin S, Ali MS, Whitmire KH, Khokhar AR. Synthesis characterization and X-ray crystal structures of cis-1,4-diaminocyclohexane-platinum(II) nucleobase adducts. Polyhedron 2007;26:637–44.
[24] Ranaldo R, Margiotta N, Intini FP, Pacifico C, Natile G. Conformer distribution in (cis-1,4-DACH)bis(guanosine-5′-phosphate)platinum(II) adducts: a reliable model for DNA adducts of antitumoral cisplatin. Inorg Chem 2008;47:2820–30.
[25] Brabec V, Palecek E. The influence of salts and pH on polarographic currents produced by denatured DNA. Biophysik 1970;6:290–300.
[26] Brabec V, Palecek E. Interaction of nucleic acids with electrically charged surfaces. II. Conformational changes in double-helical polynucleotides. Biophys Chem 1976;4:76–92.
[27] Brabec V, Sip M, Leng M. DNA conformational distortion produced by site-specific interstrand cross-link of trans-diamminedichloroplatinum(II). Biochemistry 1993;32:11676–81.
[28] Manley JL, Fire A, Cano A, Sharp PA, Gefter ML. DNA-dependent transcription of adenovirus genes in a soluble whole-cell extract. Proc Natl Acad Sci USA 1980;77:3855–9.
[29] Reardon JT, Vaisman A, Chaney SG, Sancar A. Efficient nucleotide excision repair of cisplatin, oxaliplatin, and bis-aceto-ammine-dichloro-cyclohexylamine-platinum(IV) (JM216) platinum intrastrand DNA diadducts. Cancer Res 1999;59:3968–71.
[30] Egger AE, Rappel C, Jakupec MA, Hartinger CG, Heffeter P, Keppler BK. Development of an experimental protocol for uptake studies of metal compounds in adherent tumor cells. J Anal Atom Spectrom 2009;24:51–61.
[31] Dabrowiak JC, Goodisman J, Souid AK. Kinetic study of the reaction of cisplatin with thiols. Drug Metab Dispos 2002;30:1378–84.
[32] Hagrman D, Goodisman J, Dabrowiak JC, Souid AK. Kinetic study on the reaction of cisplatin with metallothionein. Drug Metab Dispos 2003;31:916–23.
[33] Kim SD, Vrana O, Kleinwächter V, Niki K, Brabec V. Polarographic determination of subnanogram quantities of free platinum in reaction mixture with DNA. Anal Lett 1990;23:1505–18.
[34] Kasparkova J, Mellish KJ, Qu Y, Brabec V, Farrell N. Site-specific d(GpG) intrastrand cross-links formed by dinuclear platinum complexes. Bending and NMR studies. Biochemistry 1996;35:16705–13.
[35] Brabec V, Leng M. DNA interstrand cross-links of trans-diamminedichloroplatinum(II) are preferentially formed between guanine and complementary cytosine residues. Proc Natl Acad Sci USA 1993;90:5345–9.
[36] Brabec V, Reedijk J, Leng M. Sequence-dependent distortions induced in DNA by monofunctional platinum(II) binding. Biochemistry 1992;31:12397–402.
[37] Novakova O, Kasparkova J, Vrana O, van Vliet PM, Reedijk J, Brabec V. Correlation between cytotoxicity and DNA binding of polypyridyl ruthenium complexes. Biochemistry 1995;34:12369–78.
[38] Keck MV, Lippard SJ. Unwinding of supercoiled DNA by platinum ethidium and related complexes. J Am Chem Soc 1992;114:3386–90.
[39] Bailly C, Gentle D, Hamy F, Purcell M, Waring MJ. Localized chemical reactivity in DNA associated with the sequence-specific bisintercalation of echinomycin. Biochem J 1994;300:165–73.
[40] Ross SA, Burrows CJ. Cytosine-specific chemical probing of DNA using bromide and monoperoxysulfate. Nucleic Acids Res 1996;24:5062–3.
[41] Bailly C, Waring MJ. Diethylpyrocarbonate and osmium tetroxide as probes for drug-induced changes in DNA conformation in vitro. In: Fox KR, editor. Drug–DNA interaction protocols. Totowa/NJ: Humana Press, Inc.; 1997. p. 51–79.
[42] Koo HS, Wu HM, Crothers DM. DNA bending at adenine.thymine tracts. Nature 1986;320:501–6.
[43] Bellon SF, Lippard SJ. Bending studies of DNA site-specifically modified by cisplatin, trans-diamminedichloroplatinum(II) and cis-Pt(NH$_3$)$_2$(N3-cytosine)Cl$^+$. Biophys Chem 1990;35:179–88.
[44] Kasparkova J, Farrell N, Brabec V. Sequence specificity, conformation, and recognition by HMG1 protein of major DNA interstrand cross-links of antitumor dinuclear platinum complexes. J Biol Chem 2000;275:15789–98.
[45] Kasparkova J, Novakova O, Marini V, Najajreh Y, Gibson D, Perez J-M, et al. Activation of trans geometry in bifunctional mononuclear platinum complexes by a piperidine ligand: mechanistic studies on antitumor action. J Biol Chem 2003;278:47516–25.
[46] Novakova O, Kasparkova J, Malina J, Natile G, Brabec V. DNA–protein cross-linking by trans-[PtCl$_2$(E-iminoether)$_2$]. A concept for activation of the trans geometry in platinum antitumor complexes. Nucleic Acids Res 2003;31:6450–60.
[47] Mendelman L, Petruska J, Goodman M. Base mispair extension kinetics. Comparison of DNA polymerase a and reverse transcriptase. J Biol Chem 1990;265:2338–46.
[48] Creighton S, Bloom LB, Goodman MF. Gel fidelity assay measuring nucleotide misinsertion, exonucleolytic proofreading, and lesion bypass efficiencies. Methods Enzymol 1995;262:232–56.
[49] Goodman MF, Creighton S, Bloom LB, Petruska J, Kunkel TA. Biochemical basis of DNA replication fidelity. Crit Rev Biochem Mol Biol 1993;28:83–126.
[50] Brown JA, Newmister SA, Fiala KA, Suo Z. Mechanism of double-base lesion bypass catalyzed by a Y-family DNA polymerase. Nucleic Acids Res 2008;36:3867–78.
[51] Wang Z, Wu X, Friedberg EC. Nucleotide-excision repair of DNA in cell-free extracts of the yeast Saccharomyces cerevisiae. Proc Natl Acad Sci USA 1993;90:4907–11.
[52] Biggerstaff M, Wood RD. Assay for nucleotide excision repair protein activity using fractionated cell extracts and UV-damaged plasmid DNA. In: Henderson DS, editor. DNA repair protocols: eukaryotic systems. Totowa/NJ: Humana Press, Inc.; 1999. p. 357–72.
[53] Sales B, Calsou P. In vitro excision repair assay in Schizosaccharomyces pombe. In: Hendersson DS, editor. DNA repair protocols: eukaryotic systems. Totowa, NJ: Humana Press, Inc.; 1999. p. 327–35.
[54] Moufarij MA, Phillips DR, Cullinane C. Gemcitabine potentiates cisplatin cytotoxicity and inhibits repair of cisplatin–DNA damage in ovarian cancer cell lines. Mol Pharmacol 2003;63:862–9.
[55] Shahin S, Cullinane C, Gray PJ. Mitochondrial and nuclear DNA damage induced by sulphur mustard in keratinocytes. Chem Biol Interact 2001;138:231–45.
[56] Grimaldi KA, Bingham JP, Hartley JA. PCR-based assays for strand-specific measurement of DNA damage and repair I—strand-specific quantitative PCR. In: Henderson DS, editor. DNA repair protocols. Totowa/NJ: Humana Press, Inc.; 1999. p. 227–40.
[57] Kelland LR, Abel G, McKeage MJ, Jones M, Goddard PM, Valenti M, et al. Preclinical antitumor evaluation of bis-acetato-ammine-dichloro-cyclohexylamine platinum(IV): an orally active platinum drug. Cancer Res 1993;53:2581–6.
[58] Reedijk J. Why does cisplatin reach guanine-N7 with competing S-donor ligands avaiable in the cell? Chem Rev 1999;99:2499–510.
[59] Romero-Isart N, Vasak M. Advances in the structure and chemistry of metallothioneins. J Inorg Biochem 2002;88:388–96.

[60] Siddik ZH. Cisplatin: mode of cytotoxic action and molecular basis of resistance. Oncogene 2003;22:7265–79.
[61] Bancroft DP, Lepre CA, Lippard SJ. ^{195}Pt NMR kinetic and mechanistic studies of cis-diamminedichloroplatinum and trans-diamminedichloroplatinum(II) binding to DNA. J Am Chem Soc 1990;112:6860–71.
[62] Ohndorf UM, Rould MA, He Q, Pabo CO, Lippard SJ. Basis for recognition of cisplatin-modified DNA by high-mobility-group proteins. Nature 1999;399: 708–12.
[63] Zamble DB, Lippard SJ. The response of cellular proteins to cisplatin-damaged DNA. In: Lippert B, editor. Cisplatin. Chemistry and biochemistry of a leading anticancer drug. Zürich, Weinheim: VHCA, WILEY-VCH; 1999. p. 73–110.
[64] Malina J, Hofr C, Maresca L, Natile G, Brabec V. DNA interactions of antitumor cisplatin analogs containing enantiomeric amine ligands. Biophys J 2000;78: 2008–21.
[65] Loskotova H, Brabec V. DNA interactions of cisplatin tethered to the DNA minor groove binder distamycin. Eur J Biochem 1999;266:392–402.
[66] Kasparkova J, Zehnulova J, Farrell N, Brabec V. DNA interstrand cross-links of the novel antitumor trinuclear platinum complex BBR3464. Conformation, recognition by high mobility group domain proteins, and nucleotide excision repair. J Biol Chem 2002;277:48076–8.
[67] Kasparkova J, Novakova O, Farrell N, Brabec V. DNA binding by antitumor trans-[$PtCl_2(NH_3)$(thiazole)]. Protein recognition and nucleotide excision repair of monofunctional adducts. Biochemistry 2003;42:792–800.
[68] Ulanovsky L, Bodner M, Trifonov EN, Choder M. Curved DNA: design, synthesis, and circularization. Proc Natl Acad Sci USA 1986;83:862–6.
[69] Rice JA, Crothers DM, Pinto AL, Lippard SJ. The major adduct of the antitumor drug cis-diamminedichloroplatinum(II) with DNA bends the duplex by $\sim$40° toward the major groove. Proc Natl Acad Sci USA 1988;85:4158–61.
[70] Comess KM, Burstyn JN, Essigmann JM, Lippard SJ. Replication inhibition and translesion synthesis on templates containing site-specifically placed cis-diamminedichloroplatinum(II) DNA adducts. Biochemistry 1992;31:3975–90.
[71] Suo Z, Johnson K. DNA secondary structure effects on DNA synthesis catalyzed by HIV-1 reverse transcriptase. J Biol Chem 1998;273:27259–67.
[72] Vaisman A, Warren MW, Chaney SG. The effect of DNA structure on the catalytic efficiency and fidelity of human DNA polymerase beta on templates with platinum–DNA adducts. J Biol Chem 2001;276:18999–9005.
[73] Bassett E, Vaisman A, Havener JM, Masutani C, Hanaoka F, Chaney SG. Efficiency of extension of mismatched primer termini across from cisplatin and oxaliplatin adducts by human DNA polymerases beta and eta in vitro. Biochemistry 2003;42:14197–206.
[74] Moriarity B, Novakova O, Farrell N, Brabec V, Kasparkova J. 1,2-GG intrastrand cross-link of antitumor dinuclear bifunctional platinum compound with spermidine linker inhibits DNA polymerization more effectively than the cross-link of conventional cisplatin. Arch Biochem Biophys 2007;459:264–72.
[75] Alt A, Lammens K, Chiocchini C, Lammens A, Pieck JC, Kuch D, et al. Bypass of DNA lesions generated during anticancer treatment with cisplatin by DNA polymerase. Science 2007;318:967–70.
[76] Kartalou M, Essigmann JM. Mechanisms of resistance to cisplatin. Mutat Res 2001;478:23–43.
[77] Zhang S, Lovejoy KS, Shima JE, Lagpacan LL, Shu Y, Lapuk A, et al. Organic cation transporters are determinants of oxaliplatin cytotoxicity. Cancer Res 2006;66:8847–57.
[78] Lovejoy KS, Todd RC, Zhang SZ, McCormick MS, D'Aquino JA, Reardon JT, et al. cis-Diammine(pyridine)chloroplatinum(II), a monofunctional platinum(II) antitumor agent: uptake, structure, function, and prospects. Proc Natl Acad Sci USA 2008;105:8902–7.
[79] Behrens BC, Hamilton TC, Masuda H, Grotzinger KR, Whang-Peng J, Louie KG, et al. Characterization of a cis-diamminedichloroplatinum(II)-resistant human ovarian cancer cell line and its use in evaluation of platinum analogues. Cancer Res 1987;47:414–8.
[80] Cohen SM, Lippard SJ. Cisplatin: from DNA damage to cancer chemotherapy. Prog Nucleic Acid Res Mol Biol 2001;67:93–130.
[81] Wang D, Lippard SJ. Cellular processing of platinum anticancer drugs. Nat Rev Drug Discov 2005;4:307–20.
[82] Fuertes MA, Castilla J, Alonso C, Perez JM. Cisplatin biochemical mechanism of action: from cytotoxicity to induction of cell death through interconnections between apoptotic and necrotic pathways. Curr Med Chem 2003;10:257–66.
[83] Kartalou M, Essigmann JM. Recognition of cisplatin adducts by cellular proteins. Mutat Res 2001;478:1–21.
[84] Mamenta EL, Poma EE, Kaufmenn WK, Delmastro DA, Grady HL, Chaney SG. Enhanced replicative bypass of platinum–DNA adducts in cisplatin-resistant human ovarian carcinoma cell lines. Cancer Res 1994;54:3500–5.
[85] Johnson SW, Laub PB, Beesley JS, Ozols RF, Hamilton TC. Increased platinum–DNA damage tolerance is associated with cisplatin resistance and cross-resistance to various chemotherapeutic agents in unrelated human ovarian cancer cell lines. Cancer Res 1997;57:850–6.
[86] Hubscher U, Nasheuer HP, Syvaoja JE. Eukaryotic DNA polymerases, a growing family. Trends Biochem Sci 2000;25:143–7.
[87] Lam WC, Van der Schans EJC, Sowers LC, Millar DP. Interaction of DNA polymerase I (Klenow fragment) with DNA substrates containing extrahelical bases: implications for proofreading of frameshift errors during DNA synthesis. Biochemistry 1999;38:2661–8.
[88] Steitz TA. DNA polymerases: structural diversity and common mechanisms. J Biol Chem 1999;274:17395–8.
[89] Lone S, Romano LJ. Mechanistic insights into replication across from bulky DNA adducts: a mutant polymerase I allows an N-acetyl-2-aminofluorene adduct to be accommodated during DNA synthesis. Biochemistry 2003;42: 3826–34.
[90] Patel PH, Suzuki M, Adman E, Shinkai A, Loeb LA. Prokaryotic DNA polymerase I: evolution, structure, and "base flipping" mechanism for nucleotide selection. J Mol Biol 2001;308:823–37.
[91] Bellon SF, Coleman JH, Lippard SJ. DNA unwinding produced by site-specific intrastrand cross-links of the antitumor drug cis-diamminedichloroplatinum(II). Biochemistry 1991;30:8026–35.